Title
3D waterflood monitoring at Lost Hills with crosshole EM

Journal
The Leading Edge, 23(5)

ISSN
1070-485X

Authors
Wilt, Michael
Morea, Michael

Publication Date
2004-05-01

DOI
10.1190/1.1756840

Peer reviewed

3D waterflood monitoring at Lost Hills with crosshole EM

Publication Data

Michael Wilt
Schlumberger, Richmond, California, U.S.
and Michael Morea
ChevronTexaco Exploration & Production Company, Bakersfield, California, U.S.
Corresponding author: mwilt@slb.com

Abstract

Choose Top of pageAbstract <<Field setting and backgro...Enhanced recovery pilot.The crosswell EM method.Crosswell EM surveys at L...2001 results.2D and 3D processing.2002 results.Discussion.CITING ARTICLES

Producing oil and gas at the Lost Hills Field in central California has always been a challenge. Although the reserves are significant, production is hampered by low matrix permeability and unusual mechanical properties in the diatomite (marine mudstone/siltstone) reservoir. Since 1911 operators have struggled with methods to improve production, control local subsidence and well failure, and improve recovery that presently is projected to be less than 10%.

Permalink: https://doi.org/10.1190/1.1756840

Producing oil and gas at the Lost Hills Field in central California has always been a challenge. Although the reserves are significant, production is hampered by low matrix permeability and unusual mechanical properties in the diatomite (marine mudstone/siltstone) reservoir. Since 1911 operators have struggled with methods to improve production, control local subsidence and well failure, and improve recovery that presently is projected to be less than 10%.

ChevronTexaco is pilot testing a variety of technologies to improve both production and overall recovery at Lost Hills. In the enhanced recovery pilot a new well spacing is being tested in addition to changes in the water injection design and some new hydraulic-fracture designs. To monitor the effects of these new strategies, ChevronTexaco and Schlumberger have employed a number of technologies, one of which is crosswell electromagnetics (EM). The crosswell EM technology is attractive because of its capability to map the interwell resistivity distribution, which thus allows for convenient tracking of ongoing flooding operations as well as improved reservoir characterization.

In this article we describe the application of crosswell EM to monitoring waterflood operations at this pilot. We first look at the field problem, briefly describe the technology and finally show how it is used to characterize the water flood and track the ongoing saturation changes.

Field setting and background.

Choose Top of pageAbstractField setting and backgro... <<Enhanced recovery pilot.The crosswell EM method.Crosswell EM surveys at L...2001 results.2D and 3D processing.2002 results.Discussion.CITING ARTICLES

The Lost Hills Field is along the western margin of the San Joaquin Basin, approximately 45 miles northwest of Bakersfield, California, U.S. The field, approximately 8 miles long and 1 mile wide, is situated on a NW-SE trending asymmetric anticline that is oriented nearly parallel to the trend of the San Andreas Fault 25 miles to the west (Figure 1).

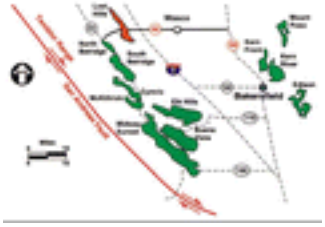

View larger version (54K)

Figure 1. Location map for San Joaquin Valley Fields.

The main productive interval is the upper Miocene Belridge Diatomite of the Monterey Formation. The Belridge Diatomite is composed of biogenic silica (skeletal remains of diatoms in the form of opal-A silica), clay, and silt/sand that combine to form interbedded diatomaceous mudstones and diatomaceous silts/sands. The mudstone is characterized by very low matrix permeability (0.1 to 1 millidarcies) whereas the siltstone is slightly more permeable (0.1 to 100 millidarcies). Porosities can range up to 65% in the mudstone and 45% in the silts/sands. Oil saturations are 40–60%, and reservoir thickness is over 1000 ft in total. This amounts to more than 2 billion barrels of oil in place.

Figure 2 shows a type log for the Belridge Diatomite at Lost Hills. The left track shows the lithology of the diatomite subdivided into three main components: clay, quartz/feldspar, and biogenic silica (opal-A). The marker track in Figure 2 represents lithologic units within this section. The units that contain a high percentage of opal-A silica (DD-E, F-FF, G-H, and J-K) are of particular interest because they have greater oil saturations and higher resistivities (2.5–6.0 ohm-m).

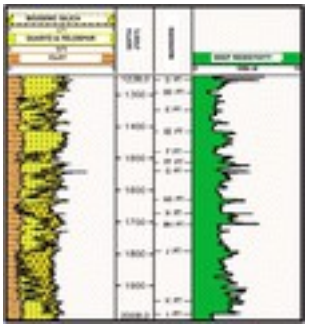

View larger version (134K)

Figure 2. Type log from Lost Hills.

Recovery operations in the Belridge Diatomite use waterflood for pressure maintenance and enhanced recovery. Production wells are sand propped and hydraulically fractured across the reservoir interval from depths of 1000–2000 ft. Injection wells are not, at present, artificially fractured, but they fracture during water injection. Average induced fracture azimuth for both producer and injection wells is N55E as determined from tiltmeter surveys.

Enhanced recovery pilot.

Choose Top of pageAbstractField setting and backgro...Enhanced recovery pilot. <<The crosswell EM method.Crosswell EM surveys at L...2001 results.2D and 3D processing.2002 results.Discussion.CITING ARTICLES

In order to address production and injection issues, the enhanced recovery (ER) pilot waterflood infill program was initiated in 2001. Four, 2.5-acre waterflood patterns in Lost Hills were converted into 16, injector-centered, 0.625-acre patterns. The northwest quarter of this pilot was selected to characterize and monitor the new flood, and in this portion of the pilot four fiberglass-cased observation wells were installed (Figure 3). The characterization efforts consisted of the acquisition of a complete suite of open hole logs and integration into the geological model for the field. In addition, core samples are available from nearby wells. Monitoring consists of repeated acquisition of induction resistivity logs in all observation wells and injection profile logs in the four injection wells. Crosswell EM surveys were made in 2001, 2002, and 2003 and are used for site characterization and pilot monitoring.

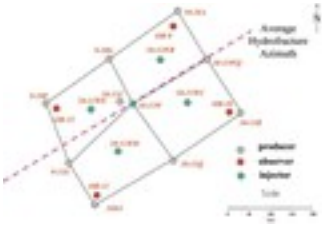

View larger version (45K)

Figure 3. Lost Hills 5⅛-acre waterflood pilot/imaging pattern.

Figure 4 shows the induction resistivity logs from the original injection well (10-11W), drilled in 1993, and nearby production well (10-11C), drilled in 2001. The apparent resistivity differences are primarily due to saturation changes associated with the water injection that has occurred during the past eight years (Rw=0.3 ohm-m). Observed changes are dominantly resistivity decreases ranging from less than 10% in the siltier intervals, to more than 40% in the diatomaceous G-H interval. In the diatomaceous intervals we estimate that a 10% decrease in resistivity corresponds approximately to an increase in water saturation of 2–3%.

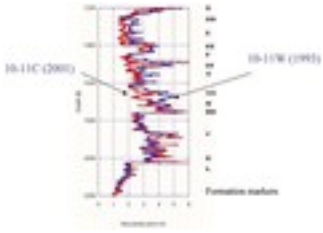

View larger version (64K)

Figure 4. Induction resistivity logs from 1995 injection well 10-11W (blue curve) and recently drilled adjacent producer 10-11C (red curve).

These logs, which are typical of logs from closely spaced wells drilled at different times in this field, suggest that resistivity changes are associated with changes in water saturation caused by flooding. This means that mapping resistivity changes, via repeated logs and crosswell measurements, might be a very effective means for tracking saturation changes during the flooding operations.

The crosswell EM method.

Choose Top of pageAbstractField setting and backgro...Enhanced recovery pilot.The crosswell EM method. <<Crosswell EM surveys at L...2001 results.2D and 3D processing.2002 results.Discussion.CITING ARTICLES

The crosswell EM method is designed to map the interwell resistivity distribution in a 2D (or 3D) sense. These data can be used to characterize reservoirs structurally and stratigraphically as well as to track ongoing processes where pore fluid is replaced or moved.

A crosshole EM field system consists of a transmitter tool in one well and a receiver tool in a second well located up to 3000 ft from the source well. The tools are connected with surface wire telemetry and deployed with standard wireline equipment. By positioning both the transmitter and receiver tools above, below, and within the zone of interest, we can collect sufficient data for a tomographic interpretation of the resistivity distribution between the wells (Figure 5). The tools are typically positioned at depth intervals equal to 5% of the well spacing, which is also roughly equal to the image resolution.

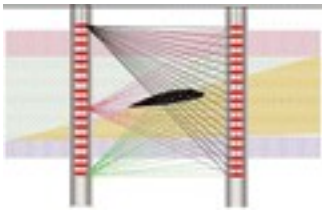

View larger version (97K)

Figure 5. Crosswell EM tomography.

Modern field instrumentation uses downhole electronics and computers for signal generation and data acquisition, which allows for very accurate and efficient data collection using standard wireline equipment. We use a small surface station for communication and power supply, and a laptop computer to control the acquisition and log the data.

The transmitter antenna is a vertical-axis magnetic core wrapped with several hundred turns of wire and tuned to broadcast a sinusoidal signal at frequencies from 1 Hz to 1 kHz. This produces a magnetic field more than 100 000 times stronger than the source of a normal induction logging system. The transmitter signal induces electrical currents to flow in the formation between the wells. These currents, in turn, generate a secondary magnetic field related to the electrical resistivity of the rock where they flow.

At the receiver borehole, we use induction coil receivers to detect the magnetic field generated by the transmitter (primary field) as well as the magnetic field from the induced currents (secondary field). The detection coils are extremely sensitive devices consisting of many thousands of turns around high permeability magnetic cores.

The system is typically configured with the receiver sensors stationary in one well while the transmitter moves between the depths of interest in the second well, broadcasting signal continuously. The receivers are then repositioned, and the process is repeated. A typical crosswell operation requires roughly 12–16 hours of field recording for a vertical section of 800 ft. Data are typically collected at a 1% error level or less.

The EM data are interpreted by computer inversion. The interwell formation is divided into two-dimensional square blocks whose sides are 2–5% of the well spacing. We apply a 2D inversion based on a finite difference forward code developed by Sandia Laboratories. Each block is assigned an electrical resistivity value, estimated from the interpolated borehole resistivity logs. The inversion code then modifies the resistivity of these blocks until the calculated and measured EM data agree to within a specified tolerance, usually related to the measurement error. This process usually requires 10–15 hours per data set on a fast computer workstation to produce a detailed image of the underground strata. The resolution of the images is roughly 2–5% of the well spacing.

We note that the images shown here are not unique. That is, we could define a different resistivity distribution that might fit the data as well. By constraining the inversions with the borehole logs and a good knowledge of the geology we reduce the uncertainty dramatically. We feel that the images shown are a good and accurate representation of the interwell resistivity distribution.

Crosswell EM surveys at Lost Hills.

Choose Top of pageAbstractField setting and backgro...Enhanced recovery pilot.The crosswell EM method.Crosswell EM surveys at L... <<2001 results.2D and 3D processing.2002 results.Discussion.CITING ARTICLES

The initial crosswell EM survey at the ER pilot was made in 2001, immediately after the drilling of the wells. We made crosshole measurements between the four observation wells (six-well pairs) over the depth interval from 1200 to 2000 ft (Figure 3). The main objective was to image the extent of the water injection plume from well 10-11W, which injected roughly 250 barrels per day for eight years prior to the survey.

Crosswell data for all six wells pairs were collected using a frequency of 350 Hz. This was a good selection because the measurements contained 30–70% secondary (formation) response but the signal level remained sufficiently high to maintain excellent quality through the 800-ft depth span. In addition data could typically be repeated to better than 0.5%, and the logging was relatively fast, about 14 hours per cross-section. We fitted all data using the 2D inversion code described above. We would typically fit a well pair, which consists of approximately 3000 individual observations to 2% or better. The inversions required 16–20 hours on a fast PC-based workstation to reach convergence.

A follow-up survey was made in 2002, approximately 18 months after the pattern changed. In this case the goal was to map the resistivity changes due both to injection and production processes. We expected these cross-sections to be more complex as there are typically 2–3 injectors or producers affecting each cross-section.

2001 results.

Choose Top of pageAbstractField setting and backgro...Enhanced recovery pilot.The crosswell EM method.Crosswell EM surveys at L...2001 results. <<2D and 3D processing.2002 results.Discussion.CITING ARTICLES

In Figure 6 we display a crosshole resistivity section from well pair OB11-OB12, which is located at the southwestern margin of the pilot. This pair trends orthogonal to the presumed fracture direction so the 2D inversion analysis is reasonably justified.

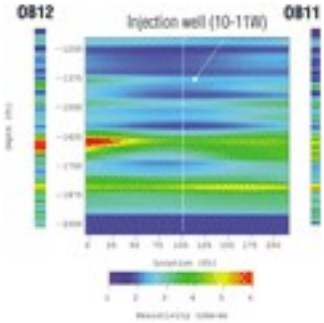

View larger version (102K)

Figure 6. Crosswell EM resistivity section between OB11 and OB12. Color-coded deep induction logs are shown at the margins.

The crosswell resistivity sections reflect the multilayered reservoir section shown in the color-coded logs, but at a smoother scale. Each section is consistent with the color-coded logs shown at the margins and neither section displays any abrupt structure with all major horizons appearing continuous. The greener and yellow intervals have a relatively high resistivity (3–6 ohm-m) and typically represent the diatomite-rich layers that are the largest producing horizons in the field. The bluer regions have a lower resistivity (1–2 ohm-m) and represent the intervening siltier intervals. The most productive diatomite intervals, designated DD, EE FF, GG-BH, and J-L, range in thickness from 10 to 100 ft, although the core analysis indicated that individual layers could be as thin as a few inches.

The color cross-section shows that the oil reservoirs at Lost Hills are an essentially flatlying layered sequence of alternating mudstone and siltstone. All of the crosswell sections are continuous and smoothly varying, so it is difficult to isolate the water-flooded zones on the basis of the resistivity.

To obtain the resistivity differences due to the waterflood we need a resistivity model of the field prior to the flood. The typical way to acquire this information is to measure crosswell data in a time-lapse mode. However, the crosswell technology was not available at this earlier time. A second method is to estimate the reservoir resistivity at the earlier time and to compare it with the measurements obtained today. This is essentially what we do.

We note the well logs collected in the observation wells at the time of drilling were very similar to logs collected in nearby parts of the field or those collected at earlier times in the same region. This suggests that the water-flooded volume has not yet affected the observation wells, which basically reflect the low permeability of the diatomite reservoir at Lost Hills. We can therefore use these logs to provide a starting model for our inversion that is unbiased by the waterflooding. As the inversion modifies the model to fit the observed data we keep track of the resistivity changes made to the model. This resistivity difference image reflects the resistivity structure unaccounted for by the

starting model but recovered by the 2D inversion. For our case, this difference mainly reflects resistivity changes related to saturation changes due to waterflooding or production.

We show one of these difference sections for well pair OB11-OB12 in Figure 7. The image delineates a zone of decreased resistivity roughly centered on the injection fracture in Well 10-11W but spreading laterally in several of the layers. The resistivity has decreased from 10 to 50% from the original model and the flooded zone extends 50–80 ft from the central fracture. We note that the largest resistivity decreases are centered on the diatomaceous horizons, which is not surprising because these zones have the highest oil saturations.

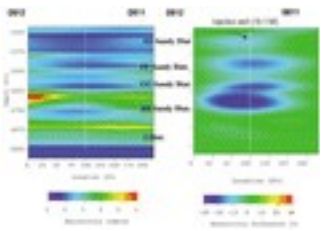

View larger version (75K)

Figure 7. Crosswell EM resistivity and difference sections between OB11 and OB12.

Whereas the injection logs showed that most of the injected water entered into the shallower horizons, EE-FF, the largest resistivity change was observed in deeper layer GG-H, a thick diatomaceous siltstone with high oil saturation. We suspect that much of the injected water communicated to this layer through the hydrofracture. We note little evidence of waterflooding into the very similar basal layer J-L; the differences in injectibility may be due to difference in local fracturing.

The narrow width of the water-swept zone after eight years of continuous water injection was initially very surprising. But if we take into consideration the large reservoir thickness, high porosity, and low permeability it is reasonable that the fluid mass did not move very far from the injection point. We also suspect that much of the initial injection was spent filling gas zones distributed within the reservoir; there could also have been some degree of fluid displacement or a small amount of dilation.

Choose Top of pageAbstractField setting and backgro...Enhanced recovery pilot.The crosswell EM method.Crosswell EM surveys at L...2001 results.2D and 3D processing. <<2002 results.Discussion.CITING ARTICLES

2D and 3D processing.

With six crosswell EM well pairs available in this limited area we can view the resistivity volume in 3D. Fortunately a 3D inverse code written by Sandia Laboratory, who also provided our 2D code, was available for use. This code is more primitive than the 2D version in terms of model preparation and data entry, and all visualization must be made using external software.

Our initial attempt at 3D imaging involved using this code and a data set reduced by about two-thirds from the 2D sections. We prepared the starting model in much the same way as before, using the interpolated logs from the observation wells as a starting guess. This 3D inversion did not in general provide satisfactory results. In several trials the inversion could achieve a good data fit by adjusting the resistivity on the fringes of the model, in volumes unrelated to the waterflood. There is clearly an issue of model equivalence in the 3D inversion. In addition the 3D inversion management tools (i.e. smoothing, starting model generation and cell lockouts) are less developed for this type of inversion than the 2D tools. A second problem was that the inversion required almost 10 days of computation time per run, making 3D data interpretation a long and tedious process and also reducing the possibility of experimentation with the code.

In the end we achieved good results by using our 2D inverse models to construct a 3D model. We found this 3D model to be consistent with the field data (using a 3D forward model to test), although our 3D inversion was not able to recover this model from the data.

In Figure 8 we show an image from this 3D model. The figure is plotted as a resistivity difference from the original starting model, based only on the logs, and shows the volume where resistivity has decreased by 15% or more during the first eight years of waterflooding.

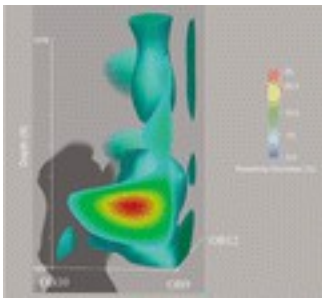

View larger version (106K)

Figure 8. Crosswell EM resistivity difference 1993–2001 at the ⅝-acre pilot.

This 3D volume of decreased resistivity is roughly centered on the central injection fracture, but it extends outward in several of the producing horizons. It never reaches more than 70 ft from the central fracture, even after eight years of water injection. The resistivity decreases at the northern end of the pilot are largely centered around a single horizon, G-BH, whereas at the southern margin there is much better depth conformance with significant flow in 3 or 4 separate reservoirs. In addition, at the southern end the width of the swept volume is narrower. What is surprising is that this variation occurs within several hundred feet along a single set of sand-propped fracture.

This type of local variation in saturation is typical of the diatomite reservoir at Lost Hills and is likely related to local fracturing. Micro fractures are evident in cores, but they are not continuous in space or time and very difficult to map. This makes it difficult to predict reservoir performance at Lost Hills based on static logs or geology.

In general, these imaging results were good news for the development of the new tightly spaced waterflood at Lost Hills. It means that there is a considerable volume of untouched reservoir within the field that could be tapped by the new wells.

Choose Top of pageAbstractField setting and backgro...Enhanced recovery pilot.The crosswell EM method.Crosswell EM surveys at L...2001 results.2D and 3D processing.2002 results.<<Discussion.CITING ARTICLES

2002 results.

The six crosswell sections were repeated in late 2002, approximately 1½ years after the onset of the pilot. We collected and interpreted the data in much the same way as the initial survey, and the data quality was the same or better, although the logging interval was slightly increased.

We show the 2002–2001 difference image from well pair OB11-OB12 in Figure 9, and the extrapolated position of the production and injection wells are also shown on the cross-section. This image is markedly different from Figure 7 in several respects. First it is more complex. The section shows significant areas where the resistivity has increased during the past 18 months as well as regions where the resistivity has decreased. The increased resistivity zones are principally located near the center of the image, and they are laminar zones roughly symmetrical about the central fracture. The resistivity decreases are associated with water injection wells, located closer to the margins of the image. We note that the resistivity increases are spread vertically throughout the section, and particularly evident in the shallower layers, whereas the resistivity decreases are more limited to depths below 1500 ft and at the margins. We note that the water injection is limited to depths below 1500 ft.

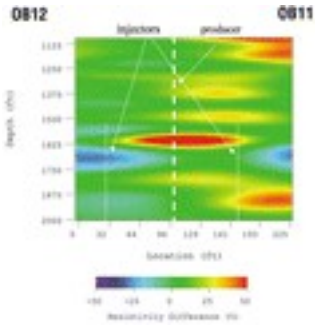

[View larger version (102K)]

Figure 9. 2001–2002 crosswell resistivity difference section between OB11 and OB12. The color-coded logs at the margins show the resistivity log difference.

We believe that the recent resistivity increase is largely production related. Although there is water injection from wells no more than 80 ft away from the producers, the low permeability does not allow the injection to resupply the reservoir at the high rate that the production is occurring. The result is a local change in the water and gas saturation, which in turn results in a net increase in resistivity. Comparing the central portion of Figures 7 and 9 we observe almost a mirror image. During the past year, virtually all the intervals that experienced resistivity declines are now seeing the resistivity increase, by a similar or somewhat larger amount. That is, the same layers that were accepting the water are now producing it.

What has proved interesting is that the wells drilled into the injection fractures are good oil producers. That is, although only water was injected into the fractures, both water and oil is being produced from the same fracture.

Discussion.

Choose Top of pageAbstractField setting and backgro...Enhanced recovery pilot.The crosswell EM method.Crosswell EM surveys at L...2001 results.2D and 3D processing.2002 results.Discussion.<<CITING ARTICLES

In general, the results of the crosswell EM are good news for the future of the 5/8;-acre pilot. For example, in the 2002 data we observed a much better vertical conformance with the earlier data, indicating that much more of the reservoir is involved in the injection and production.

The crosshole EM has provided a valuable tool to track the progress of a waterflood. Interwell resistivity changes were clearly associated with water injection just as increases were associated with zones of fluid production. Clearly, this presents an ideal case for the technology. The availability of closely spaced fiberglass wells, and a thick reservoir with well-defined periods of injection and production allowed us to unambiguously associate reservoir effects with the measured resistivity changes.

Cited by

Zhigang Wang, Gang Yu, Lin Zhang, Chongyang Wang, Jin Zhang, Zihao Liu. 2017. The use of time-frequency domain electromagnetic technique to monitor hydraulic fracturing. SEG Technical Program Expanded Abstracts, 1268-1273.
Abstract | PDF (1485 KB) | PDF w/Links (1492 KB) | Permissions
2017. EM Exploration Complete Session. SEG Technical Program Expanded Abstracts 2017, 1044-1273.
Abstract | PDF (51391 KB) | PDF w/Links (32632 KB) | Permissions
Chester Weiss, Hunter Knox, David Aldridge. 2016. Experiment design study in 3D DC resistivity: Adjoint sensitivities in a horizontal steel-cased borehole. SEG Technical Program Expanded Abstracts 2016, 942-947.
Abstract | PDF (3161 KB) | PDF w/Links (3175 KB) | Permissions
2016. EM Exploration Complete Session. SEG Technical Program Expanded Abstracts 2016, 846-1057.
Abstract | PDF (44504 KB) | PDF w/Links (26980 KB) | Permissions
Chester J. Weiss, David F. Aldridge, Hunter A. Knox, Kimberly A. Schramm, Lewis C. Bartel. (2016) The direct-current response of electrically conducting fractures excited by a grounded current source. *GEOPHYSICS* **81**:3, E201-E210.

Online publication date: 6-Apr-2016.
Abstract | Full Text | PDF (3697 KB) | PDF w/Links (657 KB) | Permissions
Chester J Weiss*, David F Aldridge, Hunter A Knox, Kimberly A Schramm, Lewis C Bartel. 2015. The DC response of electrically conducting fractures excited by a grounded current source. SEG Technical Program Expanded Abstracts 2015, 930-936.
Abstract | PDF (857 KB) | PDF w/Links (658 KB) | Supplemental Material | Permissions
Daniele Colombo, Gary Wayne McNeice. (2013) Quantifying surface-to-reservoir electromagnetics for waterflood monitoring in a Saudi Arabian carbonate reservoir. *GEOPHYSICS* **78**:6, E281-E297.
Online publication date: 4-Oct-2013.
Abstract | Full Text | PDF (7022 KB) | PDF w/Links (1152 KB) | Permissions
Anwar H. Bhuyian, Martin Landrø, Ståle E. Johansen. (2012) 3D CSEM modeling and time-lapse sensitivity analysis for subsurface CO^2CO2 storage. *GEOPHYSICS* **77**:5, E343-E355.
Online publication date: 8-Aug-2012.
Abstract | Full Text | PDF (2128 KB) | PDF w/Links (2212 KB) | Permissions
Daniel Colombo, Gary McNeice, Garrett Kramer. 2012. Sensitivity analysis of 3D surface-borehole CSEM for a Saudi Arabian carbonate reservoir. SEG Technical Program Expanded Abstracts 2012, 1-5.
Abstract | PDF (1984 KB) | PDF w/Links (758 KB) | Permissions
Lanfang He, Xiumian Hu, Ligui Xu, Zhanxiang He, Weili Li. (2012) Feasibility of monitoring hydraulic fracturing using time-lapse audio-magnetotellurics. *GEOPHYSICS* **77**:4, WB119-WB126.
Online publication date: 10-Jul-2012.
Abstract | Full Text | PDF (1970 KB) | PDF w/Links (689 KB) | Permissions
Per Atle Olsen. (2011) Coarse-scale resistivity for saturation estimation in heterogeneous reservoirs based on Archie's formula. *GEOPHYSICS* **76**:2, E35-E43.
Online publication date: 10-Mar-2011.
Abstract | Full Text | PDF (1803 KB) | Permissions
Noel Black, Michael S. Zhdanov. 2010. Active Geophysical Monitoring of Hydrocarbon Reservoirs Using EM Methods. Active Geophysical Monitoring, 135-159.
Crossref
Martha Lien, Trond Mannseth. (2008) Sensitivity study of marine CSEM data for reservoir production monitoring. *GEOPHYSICS* **73**:4, F151-F163.
Online publication date: 27-Jun-2008.
Abstract | Full Text | PDF (1367 KB) | Permissions
2008. References. Reservoir Geophysics, 121-124.
Abstract | PDF (61 KB) | Permissions